KAMPALA INTERNATIONAL UNIVERSITY

KIU
Journal of Science, Engineering and Technology

KJSET

Research Article

Design, Simulation, Fabrication and performance evaluation of a Scoria-Insulated, PID-controlled charcoal stove for efficient cooking

Barenti Denis Bruno, Milon Selvam Dennison*, P. Sathish Kumar

Department of Mechanical Engineering, School of Engineering and Applied Sciences, Kampala International University, Western Campus, Ishaka-Bushenyi, Uganda
bruno.barenti@studwc.kiu.ac.ug , milon.selvam@kiu.ac.ug, sathishpauto@kiu.ac.ug

**Corresponding Author: Milon Selvam Dennison, Department of Mechanical Engineering, School of Engineering and Applied Sciences, Kampala International University, Western Campus, Ishaka-Bushenyi, Uganda, https://orcid.org/0000-0002-2012-9288, milon.selvam@kiu.ac.ug*

Paper history:
Received 22 September 2025
Accepted in revised form 04 December 2025

Keywords
charcoal stove; scoria insulation; CFD; PID control; Water Boiling Test; thermal efficiency; specific fuel consumption.

Abstract

Access to clean and efficient cooking technologies remains a significant challenge in sub-Saharan Africa, where traditional charcoal stoves are characterized by low thermal efficiency, high fuel consumption, and elevated emissions. This study presents the design, modeling, fabrication, and performance evaluation of a novel scoria-insulated, PID-controlled charcoal stove aimed at overcoming these limitations. The workflow combined CAD/CFD analysis, embedded PID control of primary-air delivery, and standardized Water Boiling Tests (WBT). CFD indicated a non-linear emission response: CO mass fraction peaked at a moderate primary-air speed (0.62 m s^{-1}), while cleaner operation required maintaining high combustion temperatures (>1330 °C), underscoring the need for managed airflow rather than simply increasing draft. Thermal simulations and measurements showed steep radial attenuation with scoria insulation, enabling safe hot-core operation of a hot core while maintaining outer wall temperatures around 80 °C. Using CFD analysis, a non-linear relationship between CO emissions and primary-air speed was identified, with peak emissions occurring at moderate airflow (~0.62 m/s). This highlights the importance of managing airflow rather than merely increasing draft. Water Boiling Tests (WBT) revealed an average thermal efficiency of 34.2%, nearly double that of traditional sigiri stoves, with a specific fuel consumption of 0.098 kg of charcoal per kg of water a marked improvement over common baseline devices. The embedded PID control effectively maintained a 600 °C setpoint, demonstrating stable temperature regulation under dynamic conditions. PID-controlled scoria insulation halves charcoal use by UGX 810,000 annual saving, justifying investment via enhanced thermal efficiency. These findings indicate that integrating locally available materials with automated airflow management offers a sustainable pathway for producing affordable, high-performance cooking stoves that can significantly improve household energy use in the region.

1.0 Introduction

Solid biomass remains a central component of household energy in many regions of Africa, Asia, and Latin America, where socioeconomic and infrastructural constraints limit access to modern energy services [1,2]. Globally, more than 2 billion people lack access to clean cooking, and household air pollution contributes to millions of premature deaths each year, highlighting a persistent public health and development challenge. Recent assessments by the International Energy Agency (IEA) indicate that over 2 billion people still cook with polluting fuels and technologies, and progress has stagnated or reversed in parts of sub-Saharan Africa as population growth outpaces gains in access [3,4]. The World Health Organization (WHO) attributes approximately 3.2 million deaths in 2020 to household air pollution, with more than 2.1 billion people relying on solid or polluting fuels in 2023. Exposure disproportionately affects women and children due to the time spent near cooking areas [5,6].

Within sub-Saharan Africa’s urban and peri-urban centers, charcoal is the primary cooking fuel due to its high energy density, ease of transportation and storage compared to fuel wood, and its suitability for use in compact appliances [1,7]. However, charcoal’s supply chain is often environmentally and climatically damaging [8,9]. Traditional earth-mound and pit kilns typically have low conversion efficiencies, ranging from 8-12%, resulting in substantial energy losses and a high demand for feedstock to produce a given mass of fuel. Studies at both the regional and global levels have shown that charcoal production contributes to deforestation and greenhouse gas emissions. For example, modeling work and national assessments have linked charcoal demand to forest degradation and increased climate forcing, with sectoral emissions projected to increase without policy and technology interventions. interventions [10,11].

In Uganda, various surveys and research studies have consistently shown that charcoal remains the primary cooking fuel in urban areas, including Kampala, where its use is still widespread among households. Data from national census microdata and sectoral reviews indicate that cities and towns rely heavily on biomass for cooking due to its affordability, availability, and perceived reliability compared to electricity or liquefied petroleum gas (LPG) under local conditions [12,13]. This pattern of demand, combined with the low efficiency of conventional cooking devices, creates a cycle of high household fuel expenditure, environmental pressure, and poor indoor air quality.

From a technology perspective, decades of cookstove research have shown that the design of the stove, airflow management, and insulation play a significant role in determining thermal efficiency and emissions. Standardized methods, such as the Water Boiling Test and the ISO 19867-1 laboratory protocol, have been developed to measure energy and pollutant performance, allowing for comparisons across different stove categories and guiding the development of new products and policy targets [14]. Laboratory tests of numerous stove designs have revealed significant variations in fuel usage and emissions among "traditional," "rocket," "gasifier," and forced-draft stoves, emphasizing the importance of carefully selecting design features that are tailored to specific types of fuel and local contexts [15].

Despite sustained efforts, conventional charcoal stoves commonly used in Uganda, such as the metallic sigiri, have been found to have low thermal efficiencies. These stoves typically operate at efficiencies of around or below 20-25% in baseline assessments. Furthermore, they emit high levels of pollutants during real-world use[16,17]. The main reasons for these shortcomings are incomplete combustion and significant heat losses. Incomplete combustion occurs due to insufficient mixing and oxygen supply in the combustion and post-flame zones. Consequently, the stoves' poorly insulated housings and suboptimal pot-stove coupling contribute to heat losses. As a result, households end up consuming more fuel for a given cooking task. This not only degrades indoor air quality but also poses health risks due to elevated CO and PM emissions [18,19]. High charcoal consumption also amplifies pressure on forest resources and increases household energy expenditure in low-income settings, where fuel costs are a significant share of disposable income [20]. Existing "improved" devices often address only one aspect of the problem. For example, they may add insulation without also controlling the air flow precisely, or introduce secondary air without ensuring robust heat containment. As a result, they can lead to inconsistent improvements in both efficiency and emissions. Meanwhile, studies on adoption emphasize that performance improvements must be reliable, durable, and affordable in order to be sustained in practice. The main technical requirement is a charcoal stove design that combines effective insulation with controlled airflow. This is necessary to support hot, clean, and stable combustion while minimizing heat loss to the environment and allowing users to adjust the power output to suit different cooking tasks [21]. To strengthen flow across related themes, this work treats thermal simulation, liner material selection, and wall-temperature targets as a single coupled design problem informing the same efficiency-and-safety objective.

The Water Boiling Test (WBT) is a widely used laboratory method for evaluating the thermal efficiency, fuel consumption, and emissions of various devices under controlled conditions [22,23]. The ISO 19867-1:2018 standard provides a framework for harmonizing laboratory test sequences and reporting across different aspects, including efficiency, carbon monoxide (CO) and particulate matter (PM) emissions, safety, and durability. This standard enables the comparison of performance levels among different clean-cooking solutions [14]. Comparative studies, such as the 50-stove laboratory study, have shown that improved designs can significantly reduce fuel use and CO emissions compared to traditional devices. For instance, rocket-type charcoal stoves have been found to consume less energy and produce at least half the amount of CO emissions as baseline technologies in task-based tests. However, it is essential to note that the performance of these devices remains specific to their design and the type of fuel used [24].

Thermal insulation in biomass stoves reduces heat loss through conduction and convection, increases the temperature inside the chamber, and promotes the complete oxidation of CO to CO_2. Reviews of biomass-stove design converge on insulation and heat-transfer optimization as key levers, alongside pot stove coupling and flow path management, to maximize useful energy delivery [21]. In many contexts, low-cost, locally available materials are prioritized, and volcanic scoria is a material worth considering. It is lightweight, porous, and has low thermal conductivity when used as an aggregate or filler, as documented in building-materials literature. Recent studies have reported that scoria-enhanced composites have a thermal conductivity of approximately 0.16-0.20 W/m-K, which is lower than that of ordinary concrete. This supports the idea that scoria can act as a thermal barrier in applications that require heat retention and user safety near hot surfaces [25]. Taken together, the simulation-guided airflow choices and scoria-based lining aim to retain heat, lower external wall temperatures, and improve user safety without adding cost-prohibitive materials.

Air staging and secondary-air injection have been shown to influence both efficiency and emissions by separating fuel-rich pyrolysis/gasification from fuel-lean burnout zones, enhancing mixing and oxidation of CO and soot precursors. Laboratory studies have demonstrated that well-designed secondary-air injection can reduce PM and CO mass emissions, but careful optimization is necessary to avoid trade-offs, such as increased ultrafine particle numbers or excessive cooling of the flame zone. [26, 26]. Forced-draft concepts, including jets of primary air and combined primary/secondary strategies, have consistently shown lower emissions and improved thermal performance compared to natural-draft baselines when implemented with suitable flow rates and injection geometries. [27, 28].

Computational and experimental analyses emphasize the importance of secondary-air position, temperature, and flow fraction in controlling post-flame oxidation and heat-release patterns in small-scale biomass appliances [29]. These principles align with combustion science from larger-scale systems (e.g., wood stoves, boilers), where air staging is widely used to suppress NO_x and improve burnout, even if cross-scale extrapolation requires care due to geometry, fuel, and Reynolds-number differences [30]. For clarity, these airflow strategies are considered alongside liner selection and wall-temperature management as one integrated thermal/combustion design thread. Most cookstoves are open-loop devices with user-set dampers or basic airflow controls. In contrast, thermal systems typically use closed-loop controllers, particularly PID controllers, to regulate temperature around a setpoint despite disturbances. Research has shown that well-tuned PID or PID variant controllers can reduce overshoot, shorten settling time, and stabilize temperature, ultimately improving both process efficiency and product quality [31].

For small-scale, cost-sensitive applications, microcontroller-based PID systems have been demonstrated in temperature-control case studies and laboratory bench setups. These systems, which often use Arduino-class microcontrollers, have been validated with thermocouple sensing and MOSFET-driven actuators (fans/heaters) under limited hardware budgets [32].

In larger biomass systems, such as grate boilers, advanced control and optimization strategies have been implemented. These strategies, which include model-based and emission-limiting controllers, have shown a reduction in CO emissions during partial-load operation and improved overall performance. This suggests that feedback control of air/fuel delivery can be a powerful tool for cleaner combustion, and lessons learned from these systems can be applied to smaller devices with adaptation [33,34].

Field studies and programmatic reviews in Uganda have shown that user acceptance of improved cooking devices is driven by factors such as fuel savings, lower smoke, faster cooking, and the durability of the device. However, evidence also suggests that for these devices to be effective, their performance must be consistent and reliable under real-world conditions. If locally made stoves fail to meet expected efficiency or durability standards, it can lead to a loss of trust and limit their adoption over time. Economic studies have also highlighted that improved cooking devices can help reduce household fuel spending, but the actual benefits depend on various factors, including the usage patterns of the household, the price of fuel, and the ambient air quality in the area. In some cases, improved air quality in the kitchen may not necessarily translate to overall health benefits if the ambient air quality remains poor [35,36]. Overall, the literature suggests that simply improving the hardware of cooking devices is not enough. Design choices must be made with the goal of achieving measurable and repeatable performance under laboratory and field conditions, and these improvements must also be translated into affordable and manufacturable products using regional supply chains.

Three interconnected issues arise in the Ugandan charcoal stove market. Firstly, many stoves remain poorly designed and inadequately controlled, resulting in low thermal efficiency and incomplete combustion, which leads to high levels of carbon monoxide and particulate matter. This problem persists despite decades of innovation in stove design. Secondly, while the concepts of air staging and forced-draft are well-established in research, the specific integration of locally available insulating materials, such as volcanic scoria, with controlled airflow, is not well understood for charcoal stoves used in urban East Africa.

Thirdly, closed-loop temperature control, a technique widely used in industrial settings, is rarely implemented in affordable, household-scale charcoal stoves. There is limited evidence in the literature to demonstrate that this control method can stabilize combustion temperature, prevent high levels of carbon monoxide, and improve efficiency in cost-constrained devices. To address these issues, a comprehensive approach is required that combines materials, aero thermal design, and feedback control, and evaluates performance using established protocols to ensure consistency and policy relevance[22,37,38]. This study integrates scoria-based insulation, staged/forced-draft airflow, and low-cost PID closed-loop control into a single charcoal-stove architecture validated under ISO-aligned laboratory protocols for the urban Ugandan context.

This study aimed to achieve five key objectives: (i) To design and model a charcoal stove architecture that incorporates scoria-based thermal insulation and managed primary/secondary airflow. (ii) To implement a microcontroller-based PID control loop for temperature regulation using fan-assisted air delivery and appropriate sensing. (iii) To simulate flow, temperature, and species fields to inform air-injection strategies and expected combustion regimes. (iv) To fabricate and laboratory-test the prototype under standardized protocols, measuring thermal efficiency, specific fuel consumption, burning rate, and CO emissions. (v) To compare the results to conventional devices to evaluate efficiency gains, emissions reductions, and economic implications for urban Ugandan households. These objectives align with the sector's push towards evidence-based performance tiers and scalable designs that are compatible with local manufacturing and maintenance capacity.

The scope of this study focuses on charcoal-fueled domestic cooking in urban and peri-urban areas of Uganda, where there is a high demand for compact and affordable cooking devices. The technical aspects of the study include: (a) selecting materials and designing liners that use scoria-based insulation to reduce heat loss, particularly in radial directions. (b) Configuring the aero thermal system of primary and secondary air paths, taking into account the location of air injection and the flow fraction, based on simulations and literature. (c) Using embedded control systems with PID (Proportional-Integral-Derivative) to track temperature set points by adjusting airflow. The laboratory evaluation of the devices will be conducted using standardized methods, including the WBT (Water Boiling Test) concept and ISO-aligned indicators, to measure efficiency and emissions under controlled conditions. Future work will include field trials and long-term durability testing. The economic analysis is limited to the first-order implications of measured fuel savings and task times, rather than a comprehensive market analysis. The study also acknowledges the broader social determinants of adoption, such as gender dynamics and credit access, but does not empirically analyze them in this study. The study provides a technically rigorous foundation for the development of cooking devices, covering materials, combustion, and control, which can be used for subsequent field deployment and impact evaluation in Ugandan households. The study also references clean-cooking standards and targets to frame performance reporting and implications for policy and product development.

2. Materials and Methods

A scoria-insulated, temperature-controlled charcoal cookstove was designed and fabricated using SolidWorks 2022 and ANSYS 2024 R2 CFD simulations to optimize its geometry, airflow, and thermal distribution. The primary-air supply was regulated by a PID-controlled fan, and the combustion chamber temperature was monitored by K-type thermocouples connected to an Arduino microcontroller UNO. The charcoal fuel was characterized for its higher heating value and proximate composition, and it was prepared to a uniform particle size. The performance of the cookstove was assessed using the standardized Water Boiling Test (WBT), in which fixed water volumes were heated under controlled ambient conditions. Thermal efficiency, specific fuel consumption, and burning rate were calculated from replicate trials. The research workflow consisted of four integrated stages: (a) selection and preparation of materials, including scoria for insulation and lump charcoal fuel; (b) design and three-dimensional modeling of the cookstove geometry using computer-aided design tools; (c) fabrication of the prototype using locally available materials and welding techniques; (d) simulation and experimental evaluation, encompassing CFD analysis, thermal characterization, and standardized Water Boiling Tests. This sequential approach ensured that material properties, design optimization, and performance validation were systematically linked from concept to experimental test, which is depicted in **Figure 1**.

2.1. Materials and sample description

The improved cookstove was fabricated using locally available scoria as the primary insulating material, stainless steel sheet for the combustion chamber and pot-support surfaces, and mild steel for the external casing. Scoria was selected for its low thermal conductivity and high temperature resistance, providing effective insulation between the hot combustion chamber and the external surfaces. Stainless steel was used in contact zones with flame and hot gases to ensure durability and resistance to oxidation, while mild steel was used for structural support and cost efficiency.

The fuel used in all experiments was lump charcoal, which was sourced from the same batch to minimize variability in its properties. The charcoal was dried to the ambient laboratory conditions, cleaned to remove dust and fines, and then sieved to obtain pieces of a consistent particle size. This was done to ensure uniform combustion during the experiments. Before testing, the properties of the charcoal were characterized through proximate analysis, which provided information on its moisture, ash, volatile matter, and fixed carbon content. Additionally, the higher heating value (HHV) of the charcoal was measured to be approximately 30 MJ kg-1, and this value was used in calculations of thermal efficiency.
Water boiling tests were conducted using identical 7.5 L aluminum vessels with flat bottoms. Each vessel was loaded with 5 L of water per trial. The vessels were chosen for their high thermal conductivity and standardized geometry, which is consistent with the Water Boiling Test protocol. This was done to minimize variation across replicates.

2.2. Design and modeling overview

The improved cookstove was designed using SolidWorks 2022 for three-dimensional geometric modeling. The design process prioritized compact geometry, effective insulation, and controlled airflow to optimize thermal efficiency and safety. Parametric features were applied to enable adjustment of combustion chamber dimensions, insulation thickness, and primary-air inlets. Assembly models were generated to evaluate fit, manufacturability, and integration of the fan-driven air-supply system with the combustion chamber.

Computational fluid dynamics (CFD) simulations were performed in ANSYS Fluent 2024 Student Version to analyze fluid flow, combustion, and heat transfer within the stove. The simulations focused on predicting temperature distributions, velocity fields, and combustion characteristics under varying primary-air injection rates. Governing equations for mass, momentum, energy, and species transport were solved using a finite-volume approach, with turbulence represented by the standard k–ε model and combustion modeled via the eddy dissipation concept. Transient simulations were employed to capture flame stability and trends in pollutant formation, particularly carbon monoxide emissions.

Results from CAD modeling and CFD simulations were used to refine the geometry of the combustion chamber, optimize scoria insulation thickness, and determine the range of primary-air velocities for stable and clean combustion. The integration of these digital design tools ensured that the fabricated stove combined structural stability, energy efficiency, and reduced emissions before proceeding to prototyping and experimental validation.

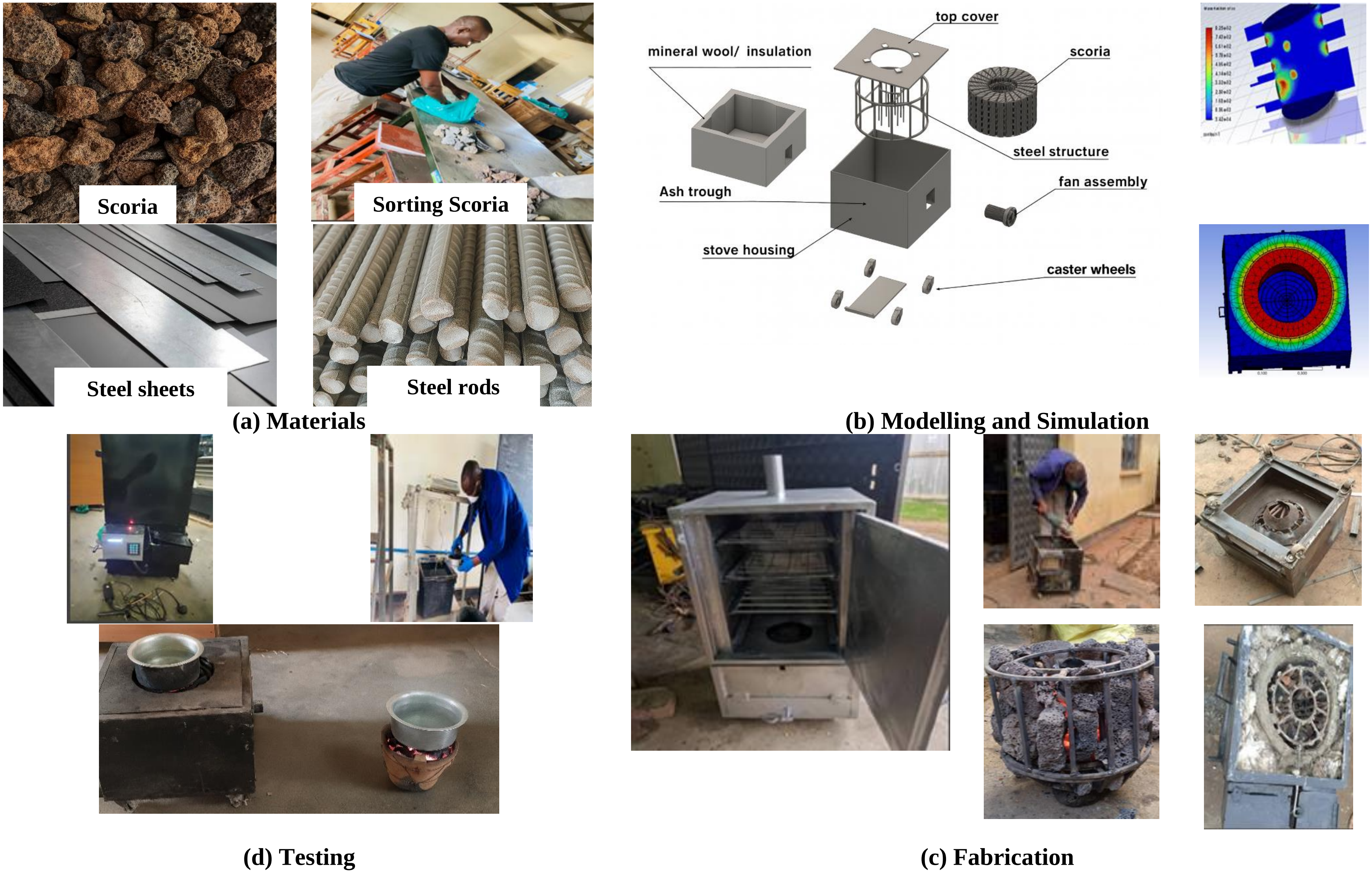

Figure 1: Process layout

2.3. Temperature sensing and PID control

Combustion chamber temperature was monitored using K-type thermocouples (Ω Engineering, USA; accuracy ±1.5 °C), positioned at representative locations within the chamber wall and gas stream. Thermocouple signals were conditioned through MAX31855 cold-junction compensation amplifiers and interfaced with an Arduino Uno R3 microcontroller (Arduino LLC, Italy) for digital acquisition. The system provided temperature readings at 1 Hz sampling frequency, sufficient to capture dynamic variations during combustion.

Primary-air supply was regulated by a 12 V DC centrifugal fan, with fan speed modulated via a Pulse-Width Modulation (PWM) signal from the microcontroller. A Proportional Integral Derivative (PID) control algorithm, implemented in the Arduino environment, adjusted airflow to maintain the desired combustion chamber temperature set-point. Controller parameters were tuned using the First-Order Plus Dead Time (FOPDT) model, derived from step-response experiments on the stove. This tuning ensured stable operation with minimal overshoot and rapid recovery from disturbances.

The integrated sensing and control system enabled real-time temperature regulation, reducing variability across tests and maintaining combustion in the optimal temperature range (>1330 °C) for clean burning. This approach provided a reproducible testing environment, facilitating a fair comparison with traditional stoves operated under uncontrolled airflow conditions.

2.4. Experimental Testing and Data Collection

The performance evaluation of the developed stove was conducted using the standardized Water Boiling Test (WBT), a widely employed method for assessing biomass cookstoves. The test allowed for the determination of key performance indicators, including thermal efficiency, specific fuel consumption (kg fuel per kg water), burning rate (g/min), cooking time, and carbon monoxide (CO) emissions. All tests were performed under controlled laboratory conditions, and replicates were included to ensure statistical reliability.

2.4.1. Fuel Analysis

A detailed analysis of the charcoal fuel was conducted to establish baseline combustion characteristics for the study. This analysis included a proximate analysis to determine the fuel's moisture content, volatile matter, and ash content. These factors influence the fuel's ignition, flame stability, and energy density. Additionally, a particle size distribution was carried out, and the results were used to calculate the pressure drop across the charcoal bed. The higher heating value (HHV) of the fuel was also measured, which quantifies the total energy released per unit mass upon complete combustion. These metrics were essential for interpreting the stove's performance outcomes, including thermal efficiency, burning rate, and emissions.

2.4.1.1. Physical Properties of Charcoal

The physical characteristics of eucalyptus charcoal were evaluated since these strongly affect combustion efficiency, airflow, and heat transfer within the stove. Moisture content was measured gravimetrically using a muffle furnace in accordance with ASTM D3173. Bulk density was obtained from the ratio of mass to volume using a 50 g sample. Particle size distribution was analyzed with a sieve shaker to ensure uniformity of feedstock, while surface characteristics were assessed to understand porosity and potential reactivity. These measurements provided critical input for decisions on combustion chamber dimensions, airflow requirements, and insulation strategies, ensuring compatibility of the fuel with the stove design.

2.4.1.2. Thermal Properties of Charcoal

The thermal properties of charcoal were investigated. The calorific value of the charcoal was determined using a bomb calorimeter in accordance with ASTM E711-87 (2012) standards. Approximately 8 g of fuel was placed in a silica crucible, connected with a nickel ignition wire, and combusted under an oxygen supply until the maximum temperature was reached. The higher heating value obtained was 30 MJ/kg for eucalyptus charcoal, consistent with published values for high-quality lump charcoal. This confirmed its suitability as a high-energy fuel for efficient household cooking applications.

2.4.2. Water Boiling Test (WBT)

The WBT is laboratory-based, standardized test protocol designed to measure the efficiency and emissions performance of cookstoves under highly controlled conditions. It served as a simplified, reproducible simulation of the high-power and low-power phases of a typical cooking process. The WBT was conducted following the Global Alliance for Clean Cookstoves guidelines. Each trial employed a 7.5 L aluminum vessel filled with 5.0 ± 0.05 L of potable water at an initial temperature of 25 ± 2 °C. Water mass was measured using a digital balance with a precision of ±1 g, while bulk water temperatures were recorded with calibrated mercury-in-glass thermometers accurate to ±0.5 °C. Ambient temperature and relative humidity were monitored to ensure consistency across replicates. The stove was charged with a pre-weighed mass of air-dried lump charcoal prepared to a uniform particle size, and the mass was re-measured at the end of the trial to calculate fuel consumption. Combustion was initiated by igniting the fuel bed, with airflow regulated using the PID-controlled fan system, and heating was continued until the mean water temperature reached 98 °C, after which the fire was allowed to extinguish naturally. Each experiment was performed in triplicate to ensure reproducibility. From the collected data, thermal efficiency was calculated as the ratio of useful heat gained by water to the chemical energy available from the fuel, specific fuel consumption was expressed as the kilograms of charcoal required to boil one kilogram of water, and burning rate was determined from the rate of fuel mass loss over time.

3. Results and Discussions

This section presents a comprehensive technical evaluation of a modern, high-efficiency biomass cookstove designed to mitigate cooking challenges. The investigation provides a quantitative analysis of key performance indicators, including thermal efficiency (η), specific fuel consumption (SFC), and burning rate. Moreover, it examines the stove’s operational characteristics through its temperature control system and internal temperature distribution. The objective is to provide robust data that validates the stove’s performance and quantifies its potential economic, health, and environmental benefits for Ugandan families compared to existing cooking technologies.

3.1. Computational fluid dynamics (CFD)

An analysis of the computational fluid dynamics (CFD) simulation was conducted to understand the effect of primary air inlet speed on the combustion process within a charcoal stove insulated with scoria. The goal was to identify optimal conditions for maximizing combustion efficiency while minimizing harmful emissions. The simulation results, detailing the relationship between primary air speed and the maximum mass fractions of carbon monoxide (CO) and carbon dioxide (CO_2), are presented.

3.1.1. Analysis of Primary Air Speeds Effect on CO Emissions

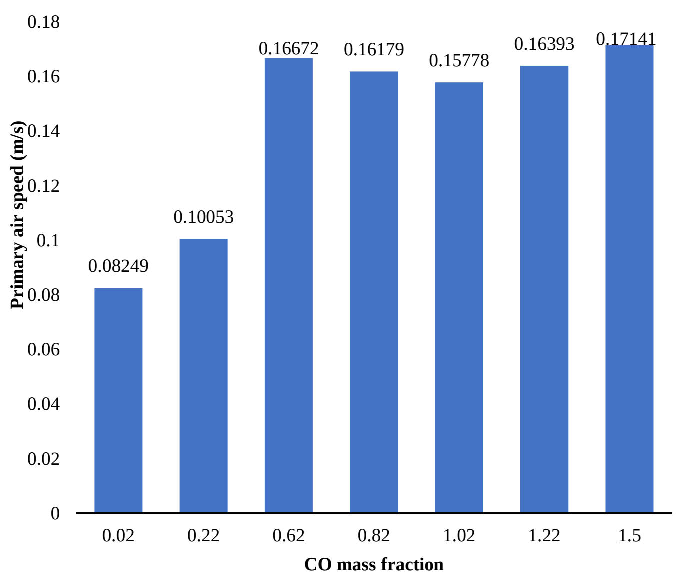

Figure 2: *Relationship between primary air speed and CO mass fraction*

.**Figure 2** shows the variation of CO mass fraction with primary-air speed. The results indicate that CO increases from approximately 0.082 at a primary-air speed of 0.02 m/s to a broad maximum of about 0.167 at a primary-air speed of 0.62-0.82 m/s. The CO levels then remain elevated with small variations (0.158-0.171) up to a primary-air speed of 1.50 m/s. This trend is non-monotonic, with a distinct high-CO region around 0.6-0.9 m/s, rather than a simple linear increase or a decrease in CO levels at higher airflow. This pattern is consistent with the combustion dynamics in biomass stoves. When the primary air supply is increased, it intensifies the devolatilization and fuel gas release, but it also shortens the residence time and lowers the post-flame temperature, which limits the conversion of CO to CO2. Without secondary air injection or enhanced mixing, the combustion zone is unable to achieve complete oxidation. The data suggest that there is a cautionary operating zone at mid-range air speeds and that clean, efficient performance requires either staged air supply or active temperature-based airflow control.

3.1.2. Effect of Exhaust Gas Fraction on Primary Air Speeds for Peak CO and CO_2

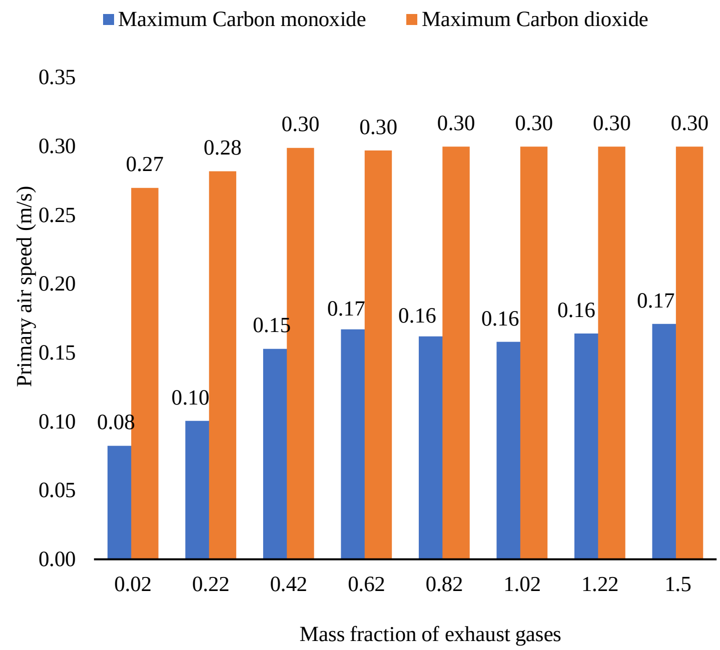

Figure 3: Primary-air speeds at which maximum CO and CO_2 concentrations occur as a function of exhaust-gas fraction. CO peaks shift to higher air speeds with increasing exhaust fraction, while CO_2 peaks remain nearly constant near 0.30 m s^{-1}

The data in **Figure 3** shows the primary-air speeds at which maximum CO and CO_2 concentrations occur as a function of the exhaust-gas fraction. It is observed that the primary-air speed at which peak CO is observed increases with an increase in the exhaust fraction. Specifically, the air speed at peak CO rises from approximately 0.085 m s^{-1} at an exhaust fraction of 0.02 to about 0.17 m s^{-1} at an exhaust fraction of 1.50. In contrast, the primary-air speed at which peak CO_2 is observed remains nearly constant at approximately 0.30 m s^{-1} once the exhaust fraction reaches 0.42 or more. This suggests that the conditions that maximize CO_2 are less sensitive to changes in the exhaust fraction within the tested range. The main inference from this data is that as the exhaust fraction increases, the primary-air speed at which peak CO is observed also increases, while the primary-air speed at which peak CO_2 is observed remains relatively constant. This pattern is consistent with a system where added exhaust dilution reduces the effective oxygen and alters the temperature-residence-time balance, resulting in the need for higher primary-air speeds to reach the CO-rich condition.

3.1.3. Effect of Primary Air Speed on Maximum Combustion Temperature

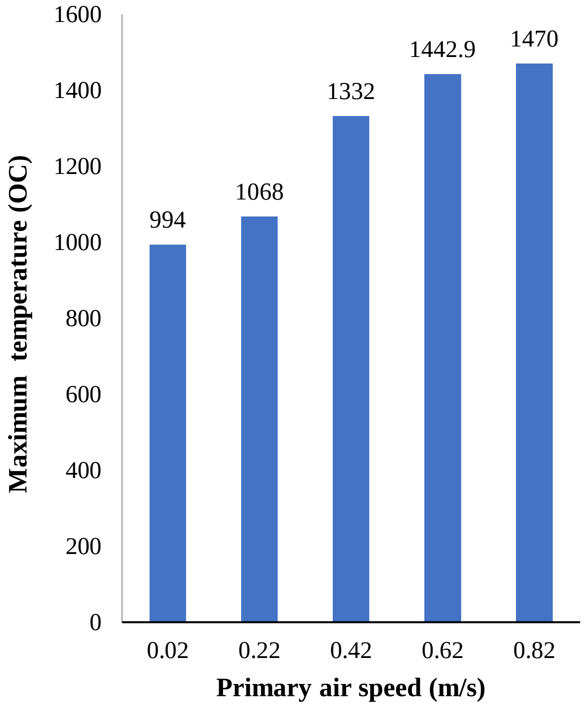

Figure 4: Relationship between primary air speed (m/s) and the corresponding maximum combustion temperature (°C)

Figure 4 demonstrates the effect of primary-air speed on the maximum combustion temperature. The results show a steady increase in peak temperature from 994 °C at a primary-air speed of 0.02 m/s to 1470 °C at 0.82 m/s. The greatest increase in temperature occurs between 0.22 and 0.42 m/s, with a rise of approximately 260 °C. After this point, the rate of temperature increase slows down, indicating that the system is approaching a thermal ceiling. At this ceiling, additional airflow results in progressively smaller gains in combustion temperature. The observed trend is consistent with combustion theory. Increasing the primary-air supply improves mixing and oxygen delivery, which promotes more complete fuel oxidation and higher flame temperatures. However, at higher air speeds, additional oxygen no longer translates directly into heat release. This is because factors such as limited fuel residence time and enhanced convective heat losses counterbalance combustion gains. The optimal operating window is between 0.62 and 0.82 m/s, where maximum temperatures above 1400 °C are achieved with stable combustion. Operating within this range is expected to improve thermal efficiency and minimize incomplete-combustion products such as CO, thereby enhancing both performance and emission control.

3.1.4. CO and CO_2 Emissions as a Function of Peak Combustion Temperature

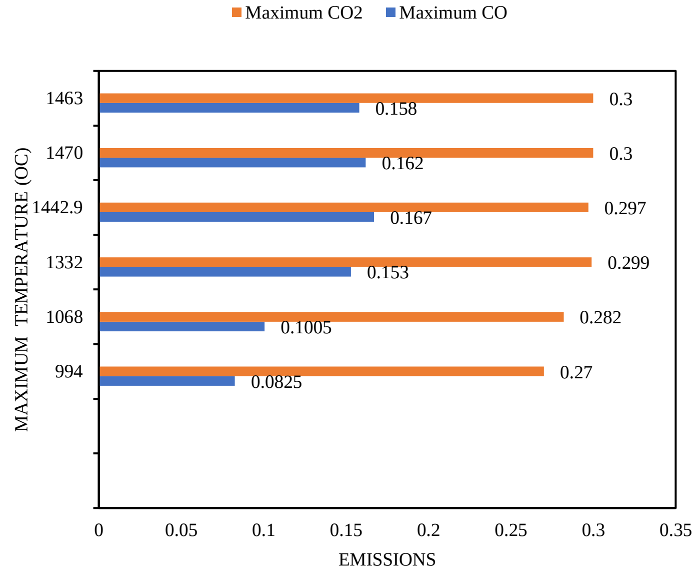

Figure 5: Relationship between maximum combustion temperatures (°C) and corresponding emissions of CO and CO_2

Figure 5 compares the mass fractions of CO and CO_2 (dimensionless) measured at various maximum combustion temperatures (approximately 994, 1068, 1332, 1442.9, 1470, and 1463 °C). The data show that CO_2 remains relatively constant across the temperature range, with a value of approximately 0.28 to 0.30. In contrast, the mass fraction of CO varies with temperature. At the two lowest temperatures (approximately 994 to 1068 °C), CO is lower, with a value of around 0.09 to 0.10. However, at the mid-to-upper temperatures (approximately 1332 to 1470 °C), CO is higher, with a value of around 0.15 to 0.17. This indicates that CO does not decrease monotonically with temperature. Instead, it is minimal at the lowest temperatures, increases at intermediate temperatures, and shows little change among the higher temperature points. The main observation is that the mass fraction of CO_2 is relatively insensitive to the tested peak temperatures, while the mass fraction of CO varies and is highest for the mid-to-high temperature cases. To understand the underlying mechanisms, such as oxygen availability, residence time, mixing, or dilution, further measurements would be required, including paired measurements of O_2, flow/air staging, and temperature fields at each condition.

3.2. Temperature Distribution

Temperature distribution in a cookstove describes how heat is spread throughout the device during operation, from the hottest point in the fire to the coolest point on the outer body. An efficient stove is designed to manage this distribution carefully to maximize cooking power while minimizing heat loss and ensuring safety.

3.2.1. Effect of Radial Distance on Temperature within the Stove's Insulating Layers

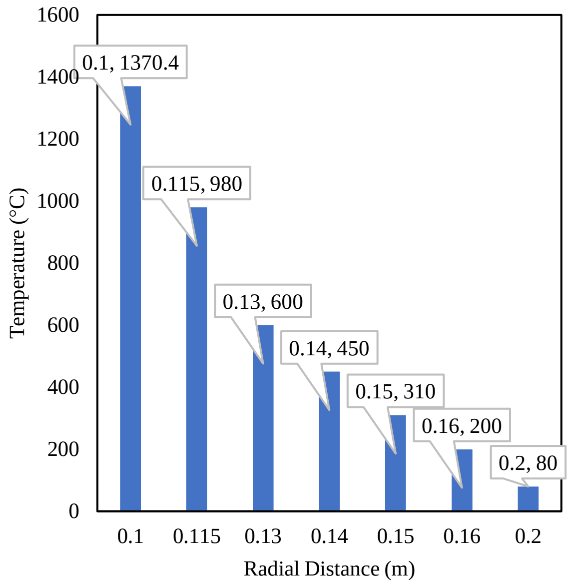

Figure 6: Radial temperature profile from the combustion zone to the outer surface under steady conditions.

Temperatures decline sharply within 0.10–0.13 m and then more gradually toward the exterior, indicating strong near-core gradients and effective attenuation through the insulating layer

Figure 6 shows the maximum temperature as a function of radial distance from the hot core. The temperature decreases from 1370.4 °C at a distance of 0.10 m to 80 °C at a distance of 0.20 m, with the greatest decrease occurring closest to the core. Over the distance of 0.10 to 0.115 m, the temperature drops by 390.4 °C, which is equivalent to a decrease of approximately 26,000 °C per meter. Over the next distance of 0.115 to 0.13 m, the temperature drops by 380 °C, which is equivalent to a decrease of approximately 25,000 °C per meter. The rate of temperature decrease then slows: over the distance of 0.13 to 0.14 m, the temperature drops by 150 °C, which is equivalent to a decrease of approximately 15,000 °C per meter; over the distance of 0.14 to 0.15 m, the temperature drops by 140 °C, which is equivalent to a decrease of approximately 14,000 °C per meter; over the distance of 0.15 to 0.16 m, the temperature drops by 110 °C, which is equivalent to a decrease of approximately 11,000 °C per meter; and over the distance of 0.16 to 0.20 m, the temperature drops by 40 °C, which is equivalent to a decrease of approximately 3,000 °C per meter. The pattern of temperature decrease is strongly non-linear, with a high rate of decrease near the core that diminishes as the distance from the core increases. This is consistent with radial conduction, where the increasing radius distributes heat over a larger area and the effective thermal resistance grows. The data indicate that the insulating layer substantially reduces the heat dissipation per meter as it approaches the exterior. However, any claims about the durability of the material or user safety should be based on separate mechanical or burn-hazard criteria and should not be inferred from this plot alone.

3.2.2. Comparative Analysis of Radial Temperature Distribution in Scoria and Clay Stoves

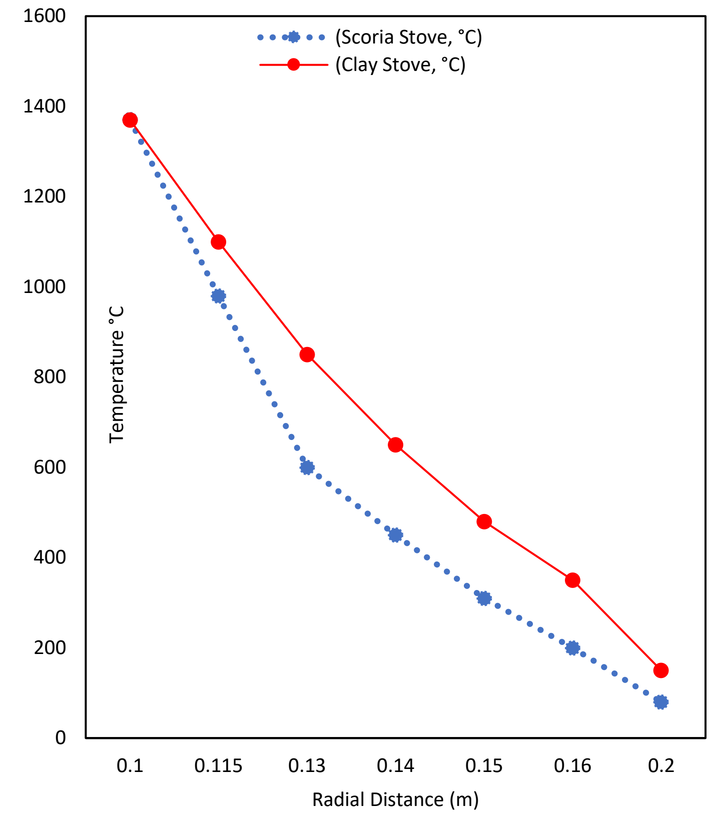

Figure 7: Comparative plot of temperature distribution with respect to radial distance (m) for Scoria and Clay Stove materials.

Figure 7 compares the radial temperature profiles of stoves lined with scoria and clay. Both profiles decrease with increasing radial distance from 0.10 to 0.20 meters, as expected for radial heat flow. At every radius shown, the scoria-lined stove is cooler than the clay-lined stove. For example, at a radius of 0.115 meters, the scoria profile is approximately 1000 degrees Celsius, while the clay profile is approximately 1100 degrees Celsius. At the outer radius of 0.20 meters, the scoria is approximately 100 degrees Celsius, whereas the clay is approximately 150-160 degrees Celsius. The steeper decline for scoria indicates stronger attenuation of heat from the core to the exterior, which is consistent with better thermal insulation performance under the tested conditions. In contrast, the higher temperatures for clay at the same radius imply greater outward heat conduction and a warmer exterior, which would increase external heat loss and potential touch-temperature risk. These inferences hold provided both liners were tested under identical geometry, thickness, and heat-release conditions. It is essential to report those parameters and uncertainties alongside the figure for reproducibility.

3.2.3. Stove Performance Comparison: Heat Transfer Efficiency

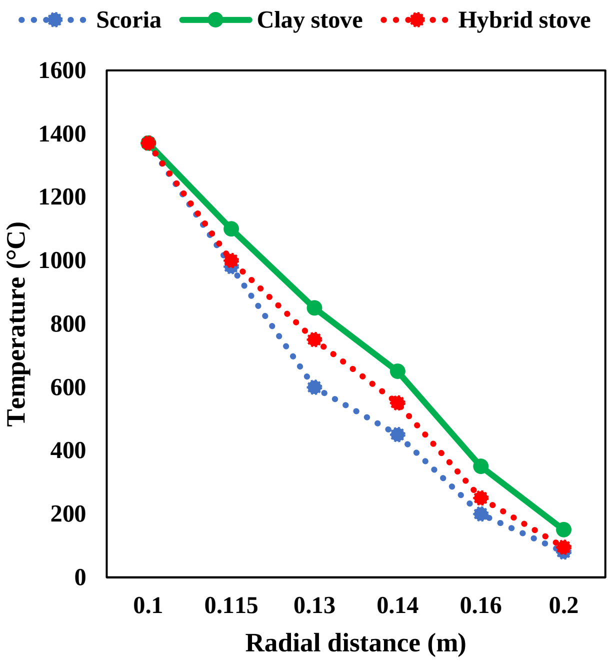

Figure 8: A comparative temperature profile for Scoria Stove, Clay Stove, and Hybrid Stove across increasing radial distances (0.1 m to 0.2 m).

Figure 8 compares radial temperature profiles for stoves lined with scoria, clay, and a hybrid lining under the same nominal operating condition. Temperatures decrease with radius for all linings (0.10–0.20 m), as expected for radial heat flow. At every radius, the clay-lined stove shows the highest temperatures, the scoria-lined stove the lowest, and the hybrid lies between them. Interpreted physically, a higher temperature at the same radius indicates greater outward heat transfer (weaker insulation) for that lining, while a lower temperature indicates stronger attenuation toward the exterior. Thus, within the tested range and assuming equal thickness/geometry, scoria provides the strongest thermal attenuation, clay the weakest, and the hybrid offers an intermediate response that is closer to clay near the core (~0.10–0.115 m) and closer to scoria near the outer wall (~0.20 m). Mechanistic attributions (specific conductivity or heat capacity values) are not established by this figure alone and should be supported by separate material property measurements or citations.

3.3. Temperature control system

A temperature control system was developed for the biomass stove to regulate combustion conditions and adapt heat output for different cooking tasks, such as boiling or simmering, by controlling the airflow through a DC fan. The system is built around an Arduino Uno microcontroller and consists of four main functional blocks: The first block is temperature sensing, which uses a thermocouple connected via an amplifier to measure the temperature. The second block is the human–machine interface, which consists of a keypad for user input and an LCD display for real-time feedback. The third block is the fan power drive, which modulates the DC fan speed to adjust the primary-air supply. The fourth block is the feedback control loop, in which the measured temperature is compared to the set-point and corrective action is applied automatically. The interconnection of these modules into a working control circuit is shown in **Figure 9.**

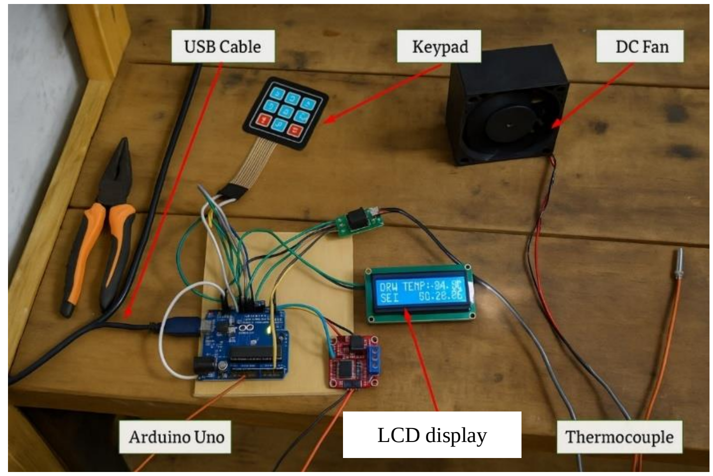

Figure 9: Temperature control system

3.3.1. Dynamic Response of the PID Temperature Control System

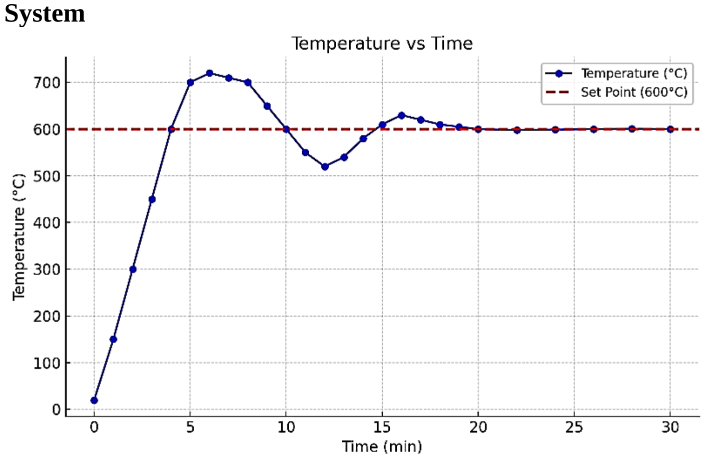

Figure 10: PID temperature control simulation for dual model stove

Figure 10 presents the simulated PID temperature control response of the hybrid stove, with a setpoint defined at 600 °C. The system exhibits a rapid temperature rise from ambient conditions, crossing the setpoint within the first 4 minutes. A substantial overshoot follows, with the temperature peaking at approximately 710°C, reflecting the aggressive proportional gain in the controller tuning. After this peak, the response enters an underdamped oscillatory phase, where the temperature fluctuates around the setpoint. The most pronounced undershoot occurs at ~520 °C near minute 11, corresponding to a deviation of about −13% from the target value.

Subsequent oscillations decrease in amplitude, demonstrating that the controller successfully damps instability over time. By approximately 20–25 minutes, the system stabilizes close to the 600 °C setpoint, with fluctuations reduced to within a narrow band (< ±5 °C). This behavior confirms that the PID parameters, while introducing significant transient oscillations, ensure reliable steady-state regulation. The results also suggest that fine-tuning, such as reducing proportional gain, increasing derivative action, or adding anti-windup measures for the integral term, could improve transient performance by limiting overshoot and shortening settling time, thereby enhancing real-time responsiveness for cooking applications.

3.4. Variation of Air Supply Ratios

In the design of high-efficiency biomass cookstoves, achieving complete combustion is the primary goal. This is managed through a two-stage air supply: primary air, which initiates combustion and gasification, and secondary air, which is crucial for burning the volatile gases and carbon monoxide (CO) produced in the first stage. The effectiveness of this process is measured by the ratio of carbon dioxide to carbon monoxide (CO_2/CO), a key indicator of combustion efficiency. A high CO_2/CO ratio signifies that the fuel has been burned completely, releasing its maximum energy, and producing fewer harmful emissions.

3.4.1. Influence of Air Staging (PA: SA Ratio) on Combustion Completeness

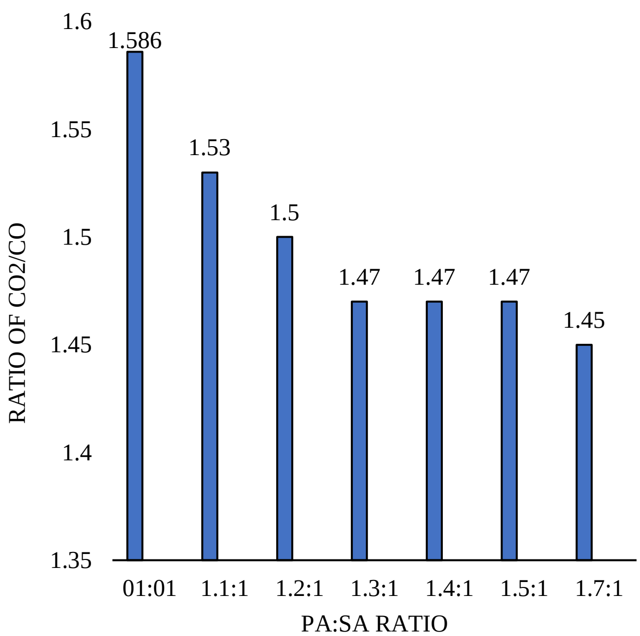

Figure 11: Relationship between the Ratio of PA: SA Ratio CO_2/CO and the CO_2/CO for various combustion conditions

Figure 11 shows the effect of primary-to-secondary air (PA:SA) staging ratio on combustion completeness, expressed as the CO_2/CO ratio. The results indicate a decline in CO_2/CO as the PA:SA ratio increases, from 1.586 at 1:0.1 to 1.45 at 1.7:1. This pattern implies that excessive secondary air supply reduces combustion efficiency by lowering flame temperature and oxygen availability in the primary reaction zone, which favors incomplete oxidation and higher relative CO levels.

Air staging is widely used to manage pollutant formation, especially to reduce thermal NO_x by separating fuel-rich and fuel-lean zones. However, in this study, higher PA:SA ratios correlate with lower CO_2/CO, showing that the benefit of NO_x suppression may come at the cost of reduced carbon burnout efficiency. The data suggest that there is an optimum balance in the secondary air fraction: modest levels can improve mixing and oxidation, whereas excessive secondary air degrades combustion completeness.

From an application perspective, the trend highlights the need for optimized PA:SA tuning in biomass and charcoal stoves. In practical settings such as Uganda, where charcoal and biomass are widely used, a low CO_2/CO ratio directly implies elevated indoor CO exposure, raising health risks for users. Thus, achieving and maintaining an optimal PA:SA ratio is essential not only for thermal efficiency but also for health and environmental outcomes.

3.5. Water Boiling Test (WBT)

A Water Boiling Test (WBT) was conducted to assess the thermal efficiency of a 2 kW scoria-insulated charcoal stove that was developed. The test compared the performance of this stove to a traditional charcoal stove. The test followed standard WBT procedures, which involve heating a known mass of water under controlled conditions to evaluate energy transfer efficiency. The test used eucalyptus charcoal as fuel, which had a measured Higher Heating Value (HHV) of 30 MJ per kilogram. For the test, 2.5 kilograms of water was placed in a metal cooking vessel at an initial temperature of 25 degrees Celsius. The amount of fuel required to bring the water to its boiling point was recorded. The developed stove consumed approximately 100 grams of charcoal to achieve boiling, which corresponds to an effective energy input of about 3.0 megajoules based on the HHV of the fuel. This performance shows that the stove can transfer a significant portion of the fuel's chemical energy into useful thermal energy for water heating. Traditional stoves typically have lower efficiencies due to higher heat losses through conduction and poor insulation. The use of scoria insulation in the developed design minimizes lateral heat loss, directing more energy upward into the cooking pot, which improves overall fuel economy and reduces charcoal consumption per cooking task.

3.6. Specific Fuel Consumption (SFC)

The SFC is a crucial metric for evaluating stove efficiency, defined as the mass of fuel required to boil or evaporate a unit mass of water. A lower SFC value indicates a more efficient stove, as it requires less fuel to perform the same task.

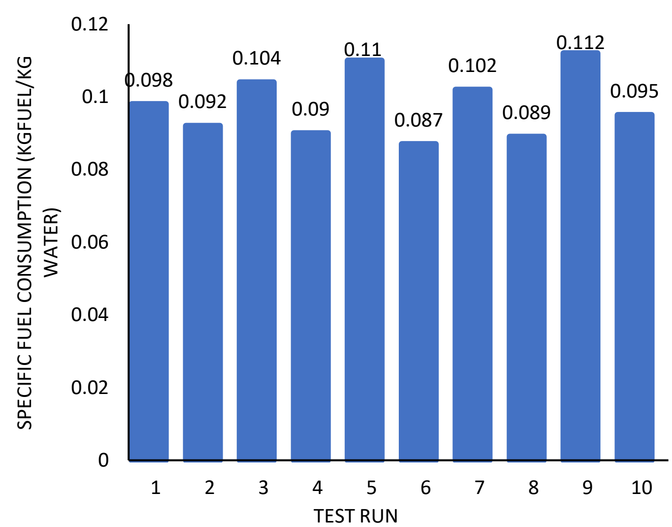

Figure 12: The Specific Fuel Consumption (SFC) of a stove over 10 different test runs.

Figure 12 presents the Specific Fuel Consumption (SFC) of the scoria-insulated stove across ten independent test runs. The results range from a minimum of 0.087 kg fuel/kg water (Test Run 6) to a maximum of 0.112 kg fuel/kg water (Test Run 9). No consistent increasing or decreasing trend is observed, and the variation instead reflects normal experimental scatter around a central value. The calculated mean SFC is 0.098 kg fuel/kg water, which provides the most representative indicator of the stove's performance under typical operating conditions.

Such fluctuations are common in combustion and water boiling tests, as small differences in fuel properties (moisture content, bulk density), operational factors (fuel loading, pot positioning), and ambient conditions (air drafts, room temperature) can influence heat transfer efficiency. Despite these natural variations, the overall stability of results suggests reliable and reproducible performance of the tested stove.

In summary, the consistently low SFC values confirm that the developed stove provides a significant performance improvement over traditional methods, combining engineering-based heat management with efficient combustion processes to achieve superior fuel economy.

3.7. Thermal efficiency

Thermal efficiency is the measure of a stove's performance and it measures the percentage of the heat from the fuel (charcoal) that gets into the stove to boil the water. The higher efficiency means lower fuel consumption.

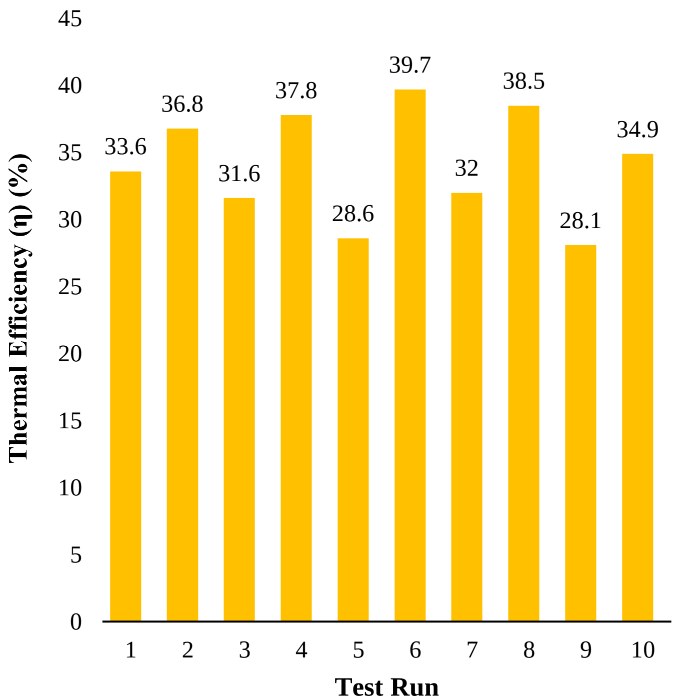

Figure 13: Thermal efficiency (η) of a stove over 10 separate test runs.

Figure 13 illustrates the thermal efficiency of the scoria-insulated charcoal stove across ten independent test runs. Efficiency values ranged from a minimum of 28.1% (Test Run 9) to a maximum of 39.7% (Test Run 6), with an average efficiency of 34.2%. This indicates that, on average, about one-third of the chemical energy contained in the charcoal was successfully converted into useful thermal energy for heating water, while the remainder was lost through convection, radiation, or incomplete combustion. The variation observed between runs is typical in biomass stove testing and reflects small differences in operational and environmental conditions, such as fuel loading, pot placement, and airflow.

3.8. Burning Rate

The burning rate is the measures of the stove's power output and how quickly it consumes fuel. It is measured in grams per minute (g/min).

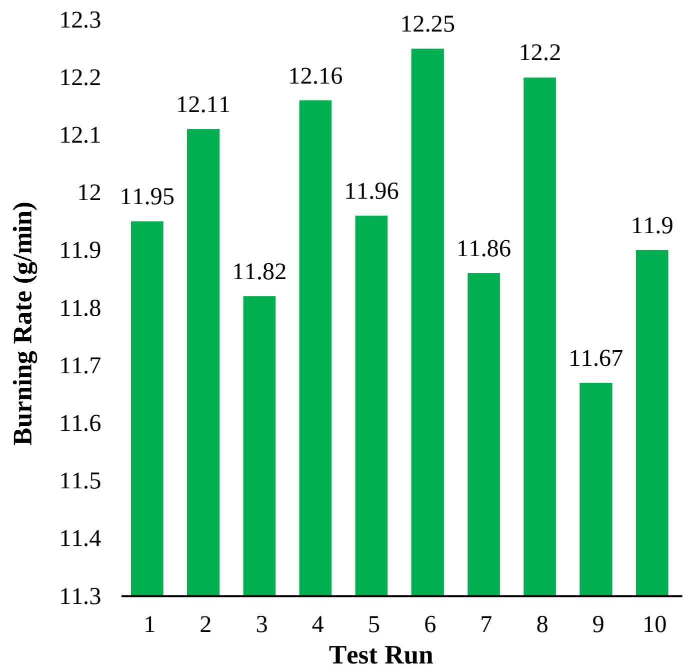

Figures 14: Burning rate of charcoal in improved stove for 10 times sample runs.

Figure 14 presents the burning rate of charcoal in the scoria-insulated stove across ten test runs. The average burning rate was 11.99 g/min, with values ranging from11.67 g/min (Run 9) to 12.25 g/min (Run 6). The results reveal a clear relationship between burning rate and fuel-use performance. The Burning Rate varies from a 11.67 (g/min) (Run 9) to a12.25 (g/min) (Run 6), with a narrow range with an average of 11.99(g/min). Conversely, run 9, with the burning rate (11.67 g/min), exhibited the peak SFC (0.112 kg/kg), indicating poorer efficiency.

This trend can be explained by combustion and heat transfer dynamics. Operating at higher burning rates aligns the stove with its optimal design air–fuel ratio, promoting more complete oxidation of carbon. A vigorous flame produces hotter, high-velocity flue gases, which enhance convective heat transfer to the cooking vessel. In addition, higher power output shortens cooking duration, reducing cumulative heat losses to the surroundings. Together, these mechanisms yield higher thermal efficiency and lower fuel demand. In practical terms, a household that would otherwise consume a 25 kg sack of charcoal per month (UGX 62,500) could achieve the same cooking output with about 15 kg of charcoal using the improved stove, saving approximately UGX 25,000 monthly (UGX 300,000 annually). Moreover, more efficient combustion reduces smoke, thereby lowering emissions of particulate matter (PM2.5) and carbon monoxide, which are linked to respiratory illnesses in women and children. Finally, reduced charcoal demand directly contributes to forest conservation and lower greenhouse gas emissions.

In summary, the data confirm that the improved stove's high burning rate coupled with low SFC reflects optimized combustion, superior thermal performance, and significant socio-environmental benefits.

3.9. Economic Analysis

Table 1: Comparative Economic Analysis of Traditional vs. Designed Stove

Variable	Traditional Stove (Sigiri)	Designed Stove	Savings
Daily Charcoal Consumption (kg)	1.5	0.75	0.75 kg per day
Cost of Charcoal (UGX per kg)	3,000	3,000	-
Daily Fuel Cost (UGX)	4,500	2,250	2,250 per day
Monthly Fuel Cost (UGX)	135,000	67,500	67,500 per month
Annual Fuel Cost (UGX)	1,620,000	810,000	810,000 per year

Table 1 presents a comparative economic analysis of the traditional charcoal stove (sigiri) and the designed scoria-insulated stove. The results clearly demonstrate the financial viability of the improved design. Daily charcoal consumption is halved, declining from 1.5 kg in the sigiri to 0.75 kg in the designed stove, resulting in a 50% reduction in fuel demand. At the prevailing market price of UGX 3,000 per kilogram of charcoal, this translates into daily fuel cost savings of UGX 2,250, monthly savings of UGX 67,500, and cumulative annual savings of UGX 810,000 per household.

These savings arise directly from the stove's superior engineering features, which combine improved thermal efficiency, optimized combustion, and active temperature control. First, the use of scoria as an insulating liner significantly reduces radial heat loss, as verified by thermal measurements showing outer casing temperatures between 80–95°C. By directing more heat vertically to the cooking vessel, less charcoal is required to achieve and maintain boiling or simmering conditions. Second, the favorable primary-to-secondary air ratio, confirmed by CO_2/CO analysis, indicates more complete combustion, meaning that a greater proportion of the fuel's chemical energy is converted into useful cooking heat. Finally, the incorporation of a PID-controlled fan system allows modulation of airflow and power output, preventing unnecessary fuel wastage during low-heat cooking tasks.

From a household economics perspective, an annual saving of UGX 810,000 represents a substantial budgetary relief, especially in low-income settings where fuel often accounts for a significant share of household expenditure. In addition, the reduced fuel demand alleviates pressure on charcoal production, thereby offering environmental benefits such as reduced deforestation and lower greenhouse gas emissions.

4. Conclusion

A scoria-integrated charcoal stove with automated temperature control was designed, simulated, fabricated, and tested, demonstrating high performance and energy efficiency for Ugandan households. CFD analysis showed a non-linear link between primary air speed and CO emissions, with optimal combustion at elevated temperatures (>1330 °C) and balanced primary–secondary air staging. Thermal simulations confirmed scoria's strong insulation core temperatures >1370 °C with outer walls near 80 °C and identified a hybrid scoria–clay liner as the best trade-off for heat concentration, safe surfaces, and reduced material stress.

An Arduino-based PID controller reached a 600 °C setpoint within minutes, exhibited transient overshoot, and stabilized within ~25 minutes, indicating effective closed-loop regulation with room for tuning. Water Boiling Tests measured 34.2% thermal efficiency and a specific fuel consumption of 0.098 kg fuel/kg water; higher combustion rates aligned with lower SFC, reflecting optimized air–fuel ratios. Economically, reduced charcoal use (≈0.75 kg/day vs. 1.5 kg/day) yields ~UGX 810,000 in annual household savings. These savings position the stove not only as an energy-efficient solution but also significantly mitigates household energy expenditure in low-income settings.

Integrating scoria insulation, optimized airflow, and PID control produced a cleaner, safer, more efficient, and more affordable charcoal stove.

4.1. Recommendations

Building on the positive results of this research, several recommendations are proposed to refine the design, strengthen its durability, and ensure successful adoption under real-world household conditions.

- The PID control algorithm should be further tuned to reduce temperature overshoot and shorten settling time, improving stability and efficiency.
- Future CFD simulations should include the effect of secondary air staging to optimize the primary-to-secondary air ratio for reducing CO emissions under all operating conditions.
- Long-term durability testing of the scoria–clay hybrid liner is needed to assess resistance to cracking, thermal stress, and material degradation during repeated daily use.
- Protective treatments or coatings should be investigated to extend the lifespan of the insulating materials under high thermal cycling.
- Extensive household field trials should be conducted to validate laboratory results under real cooking practices, providing data on fuel savings, ease of use, and cultural acceptance.
- Monitoring of indoor air quality and health outcomes during field trials will be essential to confirm the stove's potential for reducing CO exposure and respiratory risks.
- Financing mechanisms such as microcredit or targeted subsidies should be developed to overcome the higher initial capital cost of the stove.
- Community-based awareness and training programs should be promoted to highlight the stove's benefits,

including annual savings of UGX 810,000 and improved household health.

4.2. Limitations

While the study demonstrates strong technical, economic, and environmental benefits of the scoria-insulated charcoal stove, several limitations should be acknowledged to place the findings in context and guide future work.

- Laboratory-based Water Boiling Tests (WBT) were used, which may not fully represent real household cooking practices.
- The study tested only eucalyptus charcoal, so results may not extend to other charcoal types or biomass fuels.
- Long-term durability of scoria and scoria–clay liners under repeated use was not assessed.
- CFD models assumed steady-state conditions and simplified airflow, which do not capture all combustion dynamics.
- The PID control system was not fully optimized, showing overshoot and oscillations during temperature regulation.
- Economic analysis assumed constant fuel prices and cooking loads, which may vary in practice.
- Only CO and CO_2 emissions were measured; other pollutants such as PM2.5 and black carbon were not included.
- The study focused on Ugandan cooking contexts, and results may differ in other cultural or regional settings.

Funding Statement

This research received no external funding.

Data Availability Statement

All data generated or analyzed during this study are included in this article.

Declarations

Conflict of Interest: The authors declare that there is no conflict of interest regarding the publication of this paper.

Ethical Approval: Not applicable.

Consent to Participate: Not applicable.

Consent to Publish: All authors have read and approved the final manuscript and consent to its publication.

Clinical Trials: Not Applicable

Acknowledgement

The authors wish to thank Kampala International University, especially the Materials Research Laboratory, for providing the facilities that aided in the completion of this research work

References

F.Y. Malah-Kuete, Understanding the clean cooking energy access gap among developing countries: Sub-Saharan Africa vs. other developing regions, Energy 319 (2025) 135052. https://doi.org/10.1016/j.energy.2025.135052.

L. Rocha-Meneses, M. Luna-delRisco, C.A. González, S.V. Moncada, A. Moreno, J. Sierra-Del Rio, L.E. Castillo-Meza, An Overview of the Socio-Economic, Technological, and Environmental Opportunities and Challenges for Renewable Energy Generation from Residual Biomass: A Case Study of Biogas Production in Colombia, Energies 16 (2023) 5901. https://doi.org/10.3390/en16165901.

Access to clean cooking – SDG7: Data and Projections – Analysis, IEA (n.d.). https://www.iea.org/reports/sdg7-data-and-projections/access-to-clean-cooking (accessed September 12, 2025).

Executive summary – A Vision for Clean Cooking Access for All – Analysis, IEA (n.d.). https://www.iea.org/reports/a-vision-for-clean-cooking-access-for-all/executive-summary (accessed September 12, 2025).

Air pollution, (n.d.). https://www.who.int/data/gho/data/themes/air-pollution?utm_source=chatgpt.com (accessed September 12, 2025).

Household air pollution, (n.d.). https://www.who.int/news-room/fact-sheets/detail/household-air-pollution-and-health (accessed September 12, 2025).

T. Meng, W.J. Florkowski, D.B. Sarpong, M. Chinnan, A.V.A. Resurreccion, Cooking Fuel Usage in Sub-Saharan Urban Households, Energies 14 (2021) 4629. https://doi.org/10.3390/en14154629.

A.S. Bockarie, E.A. Marais, A.R. MacKenzie, Air Pollution and Climate Forcing of the Charcoal Industry in Africa, Environ. Sci. Technol. 54 (2020) 13429–13438. https://doi.org/10.1021/acs.est.0c03754.

E.N. Chidumayo, D.J. Gumbo, The environmental impacts of charcoal production in tropical ecosystems of the world: A synthesis, Energy for Sustainable Development 17 (2013) 86–94. https://doi.org/10.1016/j.esd.2012.07.004.

B. R, E. M, K. Dm, Mortality and greenhouse gas impacts of biomass and petroleum energy futures in Africa, Science (New York, N.Y.) 308 (2005). https://doi.org/10.1126/science.1106881.

E. Tazebew, S. Sato, S. Addisu, E. Bekele, A. Alemu, B. Belay, Improving traditional charcoal production system for sustainable charcoal income and environmental benefits in highlands of Ethiopia, Heliyon 9 (2023). https://doi.org/10.1016/j.heliyon.2023.e19787.

C. Drazu, M. Olweny, G. Kazoora, Household energy use in Uganda: existing sources, consumption, and future challenges, (2015).

A. Nzabona, R. Tuyiragize, J.B. Asiimwe, C. Kakuba, P. Kisaakye, Urban Household Energy Use: Analyzing Correlates of Charcoal and Firewood Consumption in Kampala City, Uganda, Journal of Environmental and Public Health 2021 (2021) 5904201. https://doi.org/10.1155/2021/5904201.

Protocols, Clean Cooking Alliance (n.d.). https://cleancooking.org/protocols/ (accessed September 12, 2025).

N. MacCarty, D. Still, D. Ogle, Fuel use and emissions performance of fifty cooking stoves in the laboratory and related benchmarks of performance, Energy for Sustainable Development 14 (2010) 161–171. https://doi.org/10.1016/j.esd.2010.06.002.

M.Z. Isah, A.M. Abioye, A.A. Fachway, structural and thermal optimization of charcoal stoves for improved efficiency and durability, Nigerian Journal of Tropical Engineering 18 (2024) 382–396. https://doi.org/10.59081/njte.18.3.009.

C. Samal, D.J. Tiwary, D. Das, S.K. Hotta, P. Ghose, G.S. Sinha, Energy, exergy and emission analysis of traditional and improved cookstoves: A comparative study, AIP Conf. Proc. 3007 (2024) 100009. https://doi.org/10.1063/5.0194087.

U. J, B. J, B. Y, B.-M. G, K. J, M. A, T. F, A.-B. K, A. P, B. N, B. S, M. N, Quantifying the Efficiency and Fuel Consumption of Cooking with Traditional Wood and Charcoal Stoves in Malawi, Ghana, and Kenya, Environmental Science & Technology 59 (2025). https://doi.org/10.1021/acs.est.5c03702.

S.A. Memon, M.S. Jaiswal, Y. Jain, V. Acharya, D.S. Upadhyay, A comprehensive review and a systematic approach to enhance the performance of improved cookstove (ICS), J Therm Anal Calorim 141 (2020) 2253–2263. https://doi.org/10.1007/s10973-020-09736-2.

A. Nzabona, R. Tuyiragize, J.B. Asiimwe, C. Kakuba, P. Kisaakye, Urban Household Energy Use: Analyzing Correlates of Charcoal and Firewood Consumption in Kampala City, Uganda, Journal of Environmental and Public Health 2021 (2021) 5904201. https://doi.org/10.1155/2021/5904201.

M.P. Kshirsagar, V.R. Kalamkar, A comprehensive review on biomass cookstoves and a systematic approach for modern cookstove design, Renewable and Sustainable Energy Reviews 30 (2014) 580–603.

P. Arora, P. Das, S. Jain, V.V.N. Kishore, A laboratory based comparative study of Indian biomass cookstove testing protocol and Water Boiling Test, Energy for Sustainable Development 21 (2014) 81–88. https://doi.org/10.1016/j.esd.2014.06.001.

K. De La Hoz C., W.A. González, Energy performance and variability of an improved top-lit updraft biomass cookstove under a water boiling test protocol, Energy Sources, Part A: Recovery, Utilization, and Environmental Effects 46 (2024) 16988–17007. https://doi.org/10.1080/15567036.2020.1819473.

N. MacCarty, D. Still, D. Ogle, Fuel use and emissions performance of fifty cooking stoves in the laboratory and related benchmarks of performance, Energy for Sustainable Development 14 (2010) 161–171. https://doi.org/10.1016/j.esd.2010.06.002.

S. Alraddadi, The impact of thermal treatment on the mechanical properties and thermal insulation of building materials enhanced with two types of volcanic scoria additives, Heliyon 9 (2023) e20814. https://doi.org/10.1016/j.heliyon.2023.e20814.

J.J. Caubel, V.H. Rapp, S.S. Chen, A.J. Gadgil, Practical design considerations for secondary air injection in wood-burning cookstoves: An experimental study, Development Engineering 5 (2020) 100049. https://doi.org/10.1016/j.deveng.2020.100049.

S. Bentson, D. Evitt, D. Still, D. Lieberman, N. MacCarty, retrofitting stoves with forced jets of primary air improves speed, emissions, and efficiency: Evidence from six types of biomass cookstoves, Energy for Sustainable Development 71 (2022) 104–117. https://doi.org/10.1016/j.esd.2022.09.013.

U. Hayyat, M.U. Khan, M. Farooq, M. Sultan, M.A. Amjed, G. Liu, X. Chunyu, F. Riaz, M. Alkhedher, Recent developments and challenges in biomass cookstove, Energy Reports 12 (2024) 2193–2208. https://doi.org/10.1016/j.egyr.2024.08.016.

U. Hayyat, G. Liu, X. Chunyu, M. Alkhedher, F. Riaz, CFD simulation of a forced draft biomass cookstove for different airflow conditions, Results in Engineering 21 (2024) 101928. https://doi.org/10.1016/j.rineng.2024.101928.

Skreiberg Oyvind, Seljeskog Morten, Kausch Franziska, Khalil Roger, Emission Levels and Emission Factors for Modern Wood Stoves, Chemical Engineering Transactions 105 (2023) 241–246. https://doi.org/10.3303/CET23105041.

J. Song, W. Cheng, Z. Xu, S. Yuan, M. Liu, Study on PID temperature control performance of a novel PTC material with room temperature Curie point, International Journal of Heat and Mass Transfer 95 (2016) 1038–1046. https://doi.org/10.1016/j.ijheatmasstransfer.2015.12.057.

P.B. de Moura Oliveira, J.D. Hedengren, E.J. Solteiro Pires, Swarm-Based Design of Proportional Integral and Derivative Controllers Using a Compromise Cost Function: An Arduino Temperature Laboratory Case Study, Algorithms 13 (2020) 315. https://doi.org/10.3390/a13120315.

L. Böhler, M. Fallmann, G. Görtler, J. Krail, F. Schittl, M. Kozek, Emission limited model predictive control of a small-scale biomass furnace, Applied Energy 285 (2021) 116414. https://doi.org/10.1016/j.apenergy.2020.116414.

C. Schörghuber, M. Gölles, M. Reichhartinger, M. Horn, Control of biomass grate boilers using internal model control, Control Engineering Practice 96 (2020) 104274. https://doi.org/10.1016/j.conengprac.2019.104274.

Improved Cookstoves Halve Air Pollution Peaks, But Ambient Exposure Dampens Health Benefits, Kleinman Center for Energy Policy (n.d.). https://kleinmanenergy.upenn.edu/research/publications/improved-cookstoves-halve-air-pollution-peaks-but-ambient-exposure-dampens-health-benefits/ (accessed September 12, 2025).

J. Ogwok, A. Naluwagga, M.S. Abbo, Uganda’s cooking energy sector: A Review, Modern Energy Cooking Services (2022).

ISO 19867-1:2018, ISO (n.d.). https://www.iso.org/standard/66519.html (accessed September 12, 2025).

ISO/TR 19867-3:2018, ISO (n.d.). https://www.iso.org/standard/73935.html (accessed September 12, 2025).